Electronic Supplementary Information

Fabrication of preferentially [001]-oriented Sb_2Se_3 thin-film on diverse substrates and its application in photoelectrochemical water reduction

Hongpeng Zhou[a], Menglei Feng[a], Peiyuan Li[a], Xiangnan Gong[c], Dingke Zhang[b]*, and Shijian Chen[a]*

[a]Chongqing Key Laboratory of Soft Condensed Matter Physics and Smart Materials, College of Physics, Chongqing University, Chongqing, 401331, China

[b]College of Physics and Electronic Engineering, Chongqing Normal University, Chongqing, 401331, China

[c]Analytical and Testing Center of Chongqing University, Chongqing 400044, China

*Corresponding author: sjchen@cqu.edu.cn; zhangdk@cqnu.edu.cn;

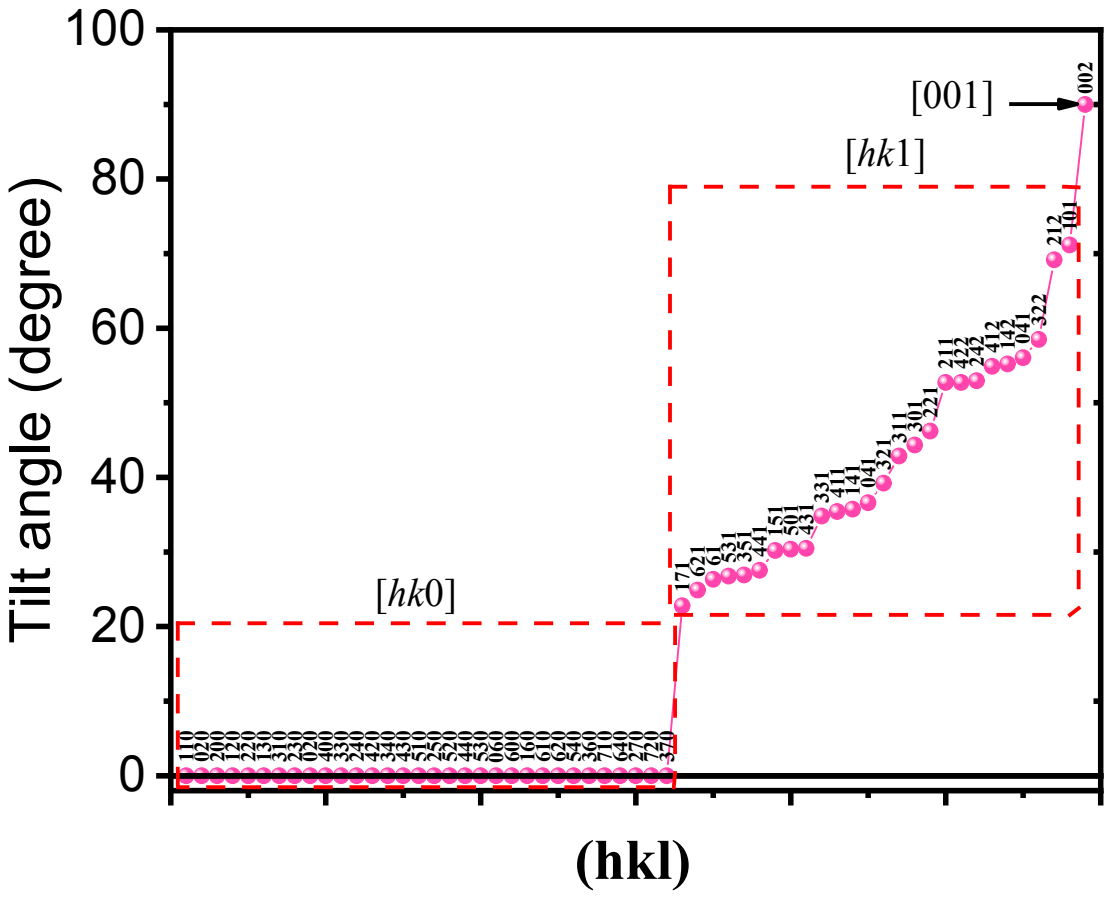

Fig. S1 The tilt angle (θ) between nanoribbon and substrate for all planes in standard XRD data (PDF No. 15-0861).

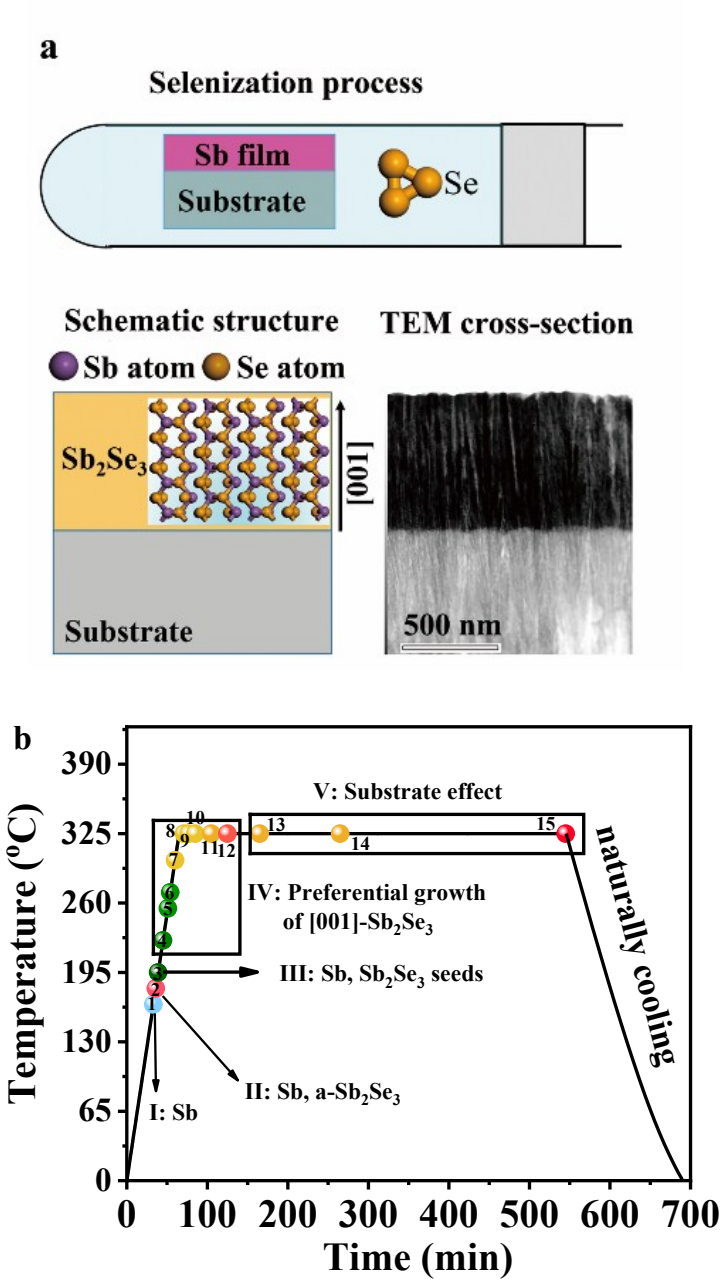

Fig. S2 (a) Synthesis of [001] preferential oriented Sb_2Se_3 via selenization in high vacuum-level (1E-4 Pa) quartz tube (11 cm^3), a schematic structure of [001] oriented Sb_2Se_3 on Mo substrate and TEM cross-section of as-prepared Sb_2Se_3/Mo film. (b) Temperature change curves used for selenization synthesis.

Table S1 The surface energy of different orientation for Sb_2Se_3.[1]

Orientation	Surface energy (J m^{-2})	
010	0.25	(hk0)
120	0.32	
110	0.33	
100	0.44	
221	0.53	(hk0)
211	0.56	
001	0.46	(00l)

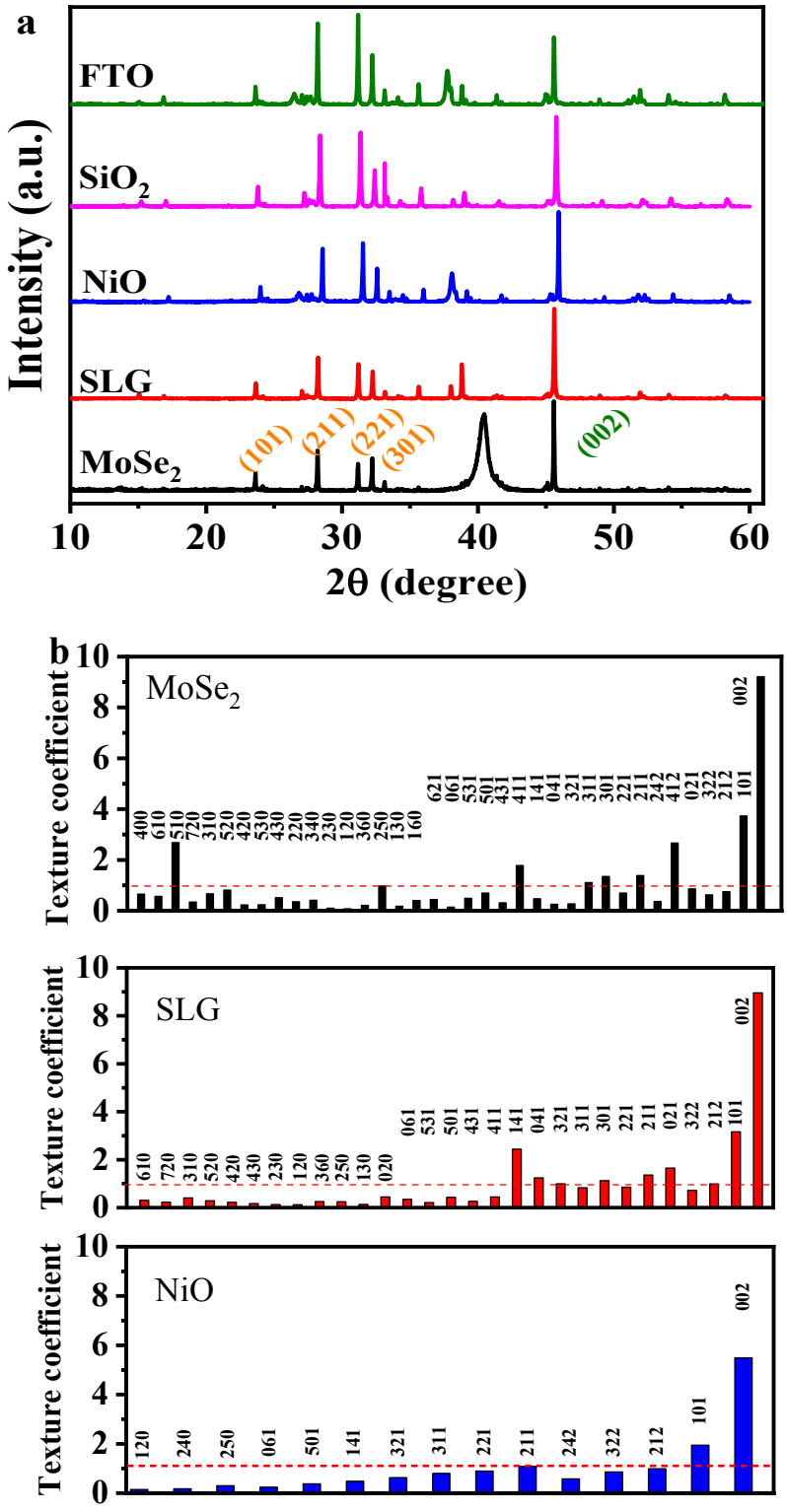
a
FTO
SiO2
NiO
SLG
MoSe2
(101)
(211)
(221)
(301)
(002)
Intensity (a.u.)
10
20
30
40
50
60
2θ (degree)
b
MoSe2
SLG
NiO
Texture coefficient
0
2
4
6
8
10

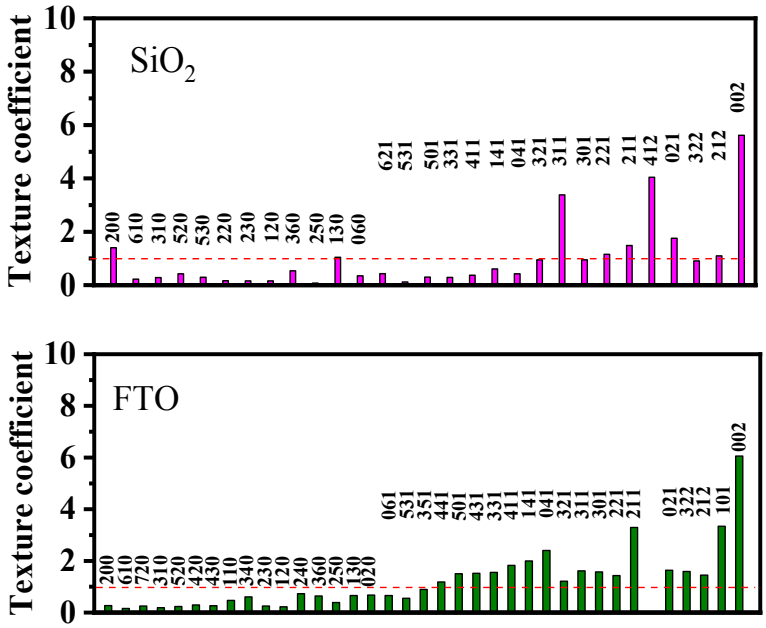

Fig. S3 Synthesis Sb_2Se_3 on the diverse substrates using selenizaiton method. (a) XRD patterns of Sb_2Se_3 (b) The texture coefficients of Sb_2Se_3 films on the diverse substrate. The (*hkl*) planes are arranged according to the tilt angle between the ribbon and the substrate plane.

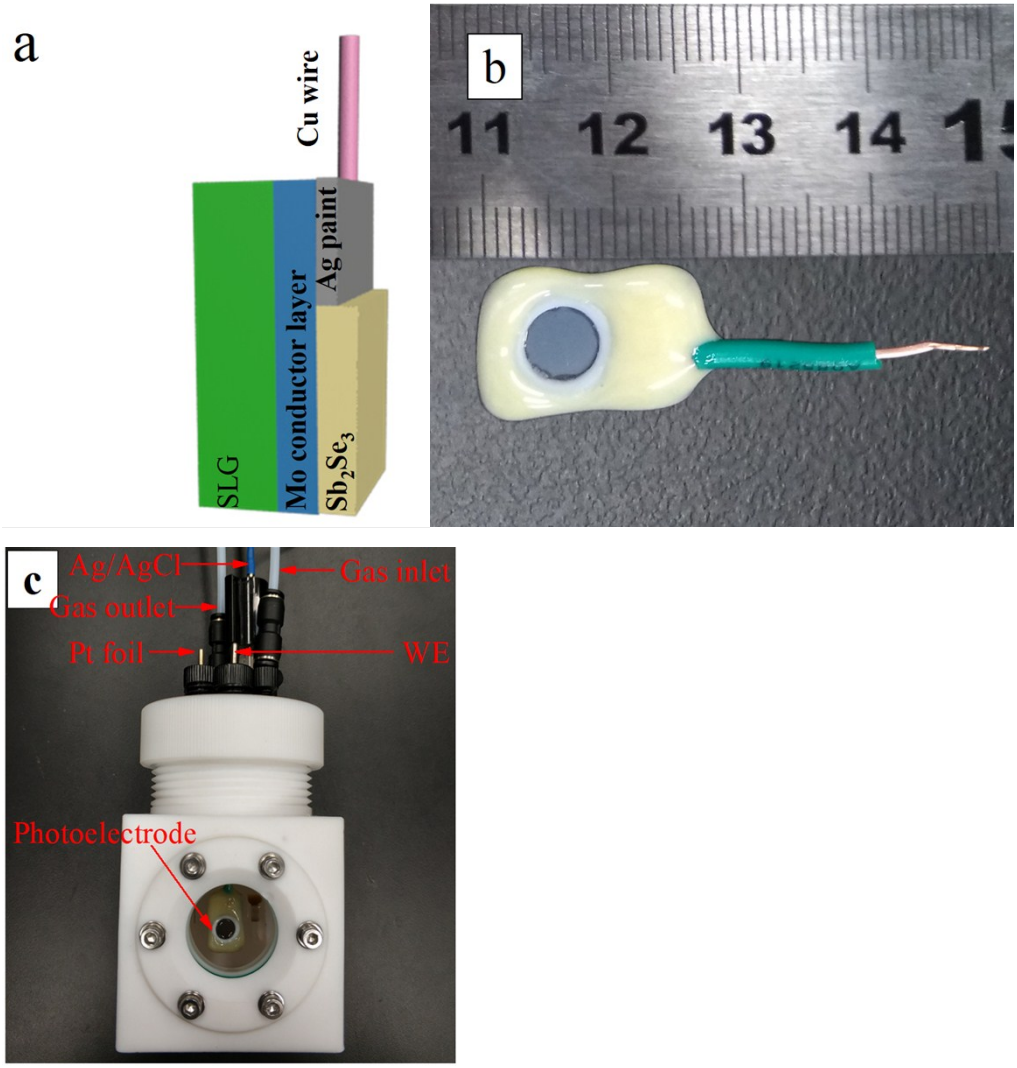

Fig. S4. (a) Schematic representation and (b) photograph of Sb_2Se_3/Mo/SLG photoelectrode with exposed Mo region connected to a copper core using silver paint, then capsulated by Loctite 9462 Hysol epoxy. (c) The set up of photoelectrochemical water splitting cell.

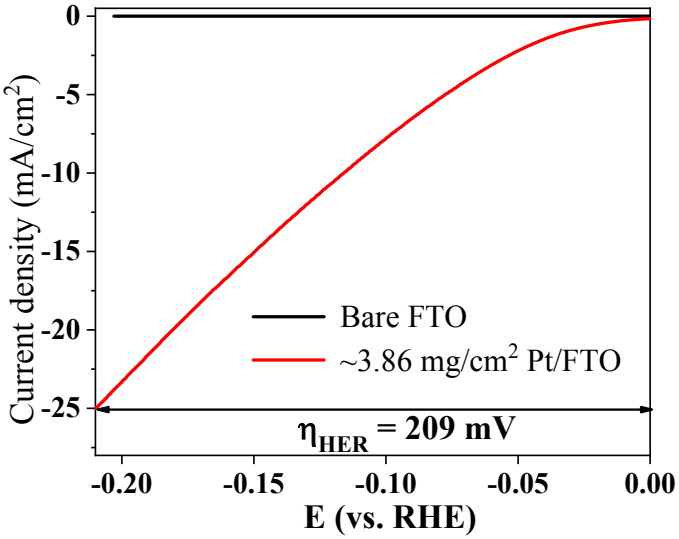

Fig. S5 LSV curves of Bare FTO glass and Pt co-catalyst on FTO glass, respectively. The conduction band of Sb_2Se_3 is known to align ~0.35 V above the H^+/H_2 redox potential.[2] Since a kinetic overpotential of only ~0.2 V is required to drive the 25 mA cm^{-2} hydrogen reduction reaction on a Pt-catalyzed surface. Thus, Pt particles loading is enough to ensure efficient surface hydrogen reduction.

Table S2 Sb_2Se_3 parameters and TiO_2 parameters for band diagram simulation.

Device	Sb_2Se_3	TiO_2
Thickness (nm)	**750**	**20**
Dielectric constant ε_r	**15**[3]	**55**[4]
Band gap Eg (eV)	**1.2**[5]	**3.2**[6]
Electron affinity χ (eV)	**4.15**[2]	**4.0**[7]
Electron mobility μ_n (cm^2 V s)	**16.9**[8]	**0.1**[9]
Hole mobility μ_h (cm^2 V s)	**2.39**[10]	**0.1**[9]
Effective conduction Band Density N_C (cm^{-3})	**2.2E20**[3]	**1E20**[4]
Effective valence Band Density N_V (cm^{-3})	**1.8E20**[3]	**1E20**[4]
Doping density (cm^{-3})	**2.0E15, acceptor***	**3E17, donor**[4]

* The donor density is determined by workfunction (5.055 eV) from scan kelvin scan microscopy (SKPM) measurement. The calculation details can be found below:

The workfunction of Sb_2Se_3 can be determined to be 5.055 eV using scan kelvin probe microscopy (SKPM). Then, the charge density can be described by the following equation:

$$N_A = N_V \exp(-\frac{E_V - E_F}{kT})$$

Where N_A and N_V (1.8E20 cm^{-3}) are acceptor density and density of states in valence band in the Sb_2Se_3. The E_v and E_F are the valence potential and Fermi energy level, respectively. The kT (0.0259 eV) is the thermal voltage. The calculation parameters are listed in table S2. The N_A was determined to be 2.0355E15.

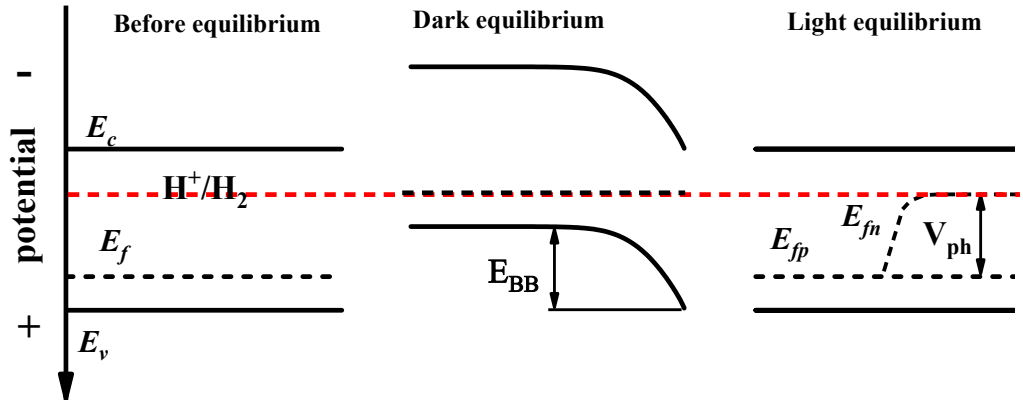

Fig. S6 Schematic diagram of maximum band bending (E_{BB}) and photovoltage (V_{ph}) for p-type semiconductor. The maximum band bending and photovoltage is equal to the difference of flat potential and redox potential before contact[11]

Table S3 Summary of PEC performance of recent reported planar Sb_2Se_3 photocathodes (orange). And Benchmarks (or typical) PEC performance of emerging earth-abundant photocathodes (green) are also listed for comparison.

Material	Device structure	pH	Current density at 0 V_{RHE} (mA/cm^2)	Reference
Reported Sb_2Se_3 photocathode	$Pt/TiO_2/Sb_2Se_3/Mo$	0.0	20.5	This work
	$Pt/TiO_2/Sb_2Se_3/NiO/FTO$	1.0	12.5	2019, ref 10
	$Pt/TiO_2/CdS/Sb_2Se_3/Mo$	6.5	8.6	2017, ref 12
	$MoS_2/Sb_2Se_3/Au/FTO$	0.0	14.2	2017, ref 13
	$Pt/TiO_2/Sb_2Se_3/Au/FTO$	1.0	30	2020, ref 14
Emerging Earth-abundant photocathode	$RuO_x/TiO_2/Ga_2O_3/Cu_2O/FTO$	5.0	10	2018, ref 15
	$Pt/TiO_2/CdS/GeSe$	6.5	10.5	2019, ref 16
	$RuO_x/TiO_2/CdS/Cu_2S/Au/FTO$	5.0	6.0	2018, ref 17
	$Pt/CdS/CuSbS_2/Mo$	6.5	4.2	2016, ref 18
	$Pt/TiO_2/CdS/CuBi_2O_4/FTO$	6.7	0.95	2017, ref 19
	$PtTiO_2/P3HT:PCBM/CuI/FTO$	1.0	8.0	2016, ref 20
	$Pt/TiO_2/ZnO/CdS/CBTS/FTO$	7	7.5	2017, ref 21

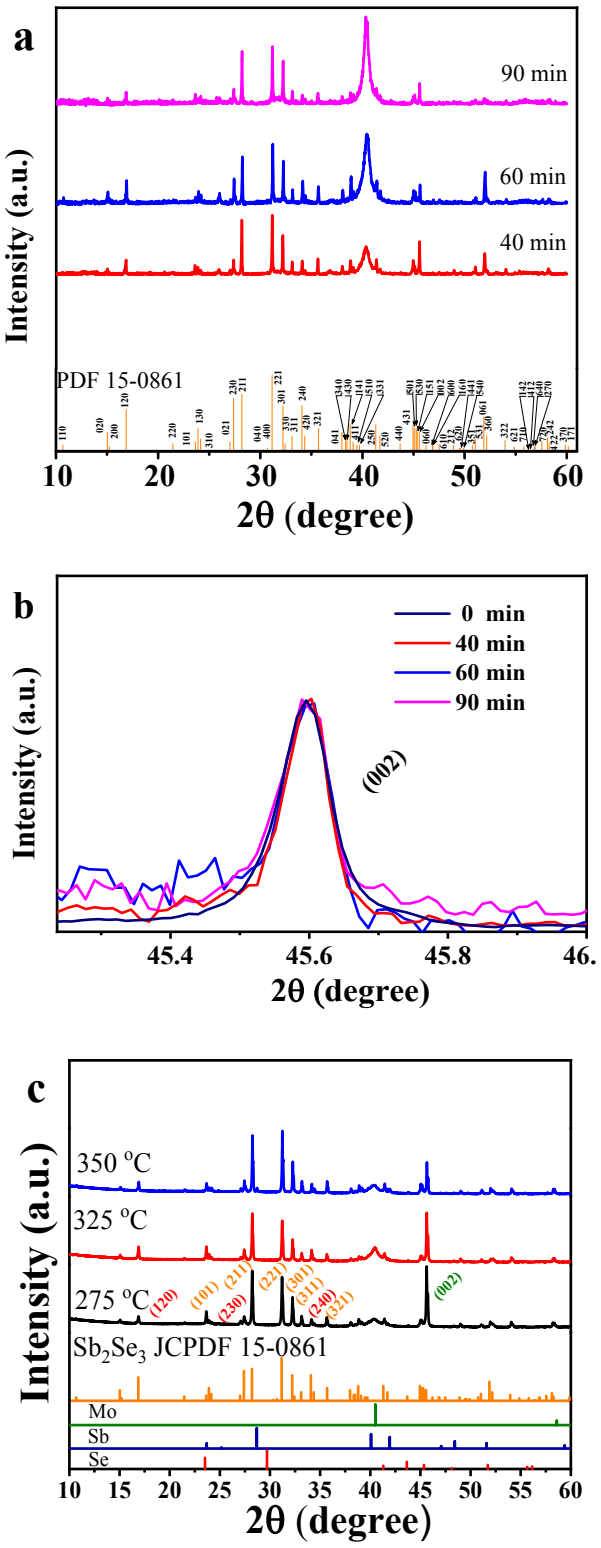

Fig. S7 (a) XRD patterns and (b) enlarged XRD patterns of preferentially [001]-oriented Sb_2Se_3 with 40, 60 and 80 min post-annealing at 500 °C. (c) The XRD patterns of Sb_2Se_3 films at different synthesis temperature using 1.0 mg Se (Please note that the Se content does not affect the results of the trend analysis). Standard diffraction data for Sb_2Se_3 (PDF No. 15-0861), Mo (PDF No. 42-1120), Sb (PDF No. 35-0732), and Se (PDF no. 86-2246) are listed for reference.

References

1. Y. Zhou, L. Wang, S. Chen, S. Qin, X. Liu, J. Chen, D.-J. Xue, M. Luo, Y. Cao, Y. Cheng, E. H. Sargent and J. Tang, *Nat. Photonics*, 2015, **9**, 409-415.
2. C. Chen, L. Wang, L. Gao, D. Nam, D. B. Li, K. H. Li, Y. Zhao, C. Ge, H. Cheong, H. Liu, H. S. Song and J. Tang, *ACS Energy Lett.*, 2017, **2**, 2125-2132.
3. L. Y. Lin, L. Q. Jiang, Y. Qiu and B. D. Fan, *J. Phys. Chem. Solids*, 2018, **122**, 19-24.
4. B. Seger, T. Pedersen, A. B. Laursen, P. C. K. Vesborg, O. Hansen and I. Chorkendorff, *J. Am. Chem. Soc.*, 2013, **135**, 1057-1064.
5. H. Zhou, M. Feng, K. Song, B. Liao, Y. Wang, R. Liu, X. Gong, D. Zhang, L. Cao and S. Chen, *Nanoscale*, 2019, **11**, 22871-22879.
6. D. O. Scanlon, C. W. Dunnill, J. Buckeridge, S. A. Shevlin, A. J. Logsdail, S. M. Woodley, C. R. A. Catlow, M. J. Powell, R. G. Palgrave, I. P. Parkin, G. W. Watson, T. W. Keal, P. Sherwood, A. Walsh and A. A. Sokol, *Nat. Mater.*, 2013, **12**, 798-801.
7. H. Zhou, Q. Chen, G. Li, S. Luo, T.-b. Song, H.-S. Duan, Z. Hong, J. You, Y. Liu and Y. Yang, *Science*, 2014, **345**, 542-546.
8. C. Chen, D. C. Bobela, Y. Yang, S. Lu, K. Zeng, C. Ge, B. Yang, L. Gao, Y. Zhao, M. C. Beard and J. Tang, *Front. Optoelectron.*, 2017, **10**, 18-30.
9. J. F. Qian, P. Liu, Y. Xiao, Y. Jiang, Y. L. Cao, X. P. Ai and H. X. Yang, *Adv. Mater.*, 2009, **21**, 3663.
10. W. Yang, J. Ahn, Y. Oh, J. Tan, H. Lee, J. Park, H. C. Kwon, J. Kim, W. Jo, J. Kim and J. Moon, *Adv. Energy Mater.*, 2018, **8**, 1702888.
11. M. S. Prevot, X. A. Jeanbourquin, W. S. Bouree, F. Abdi, D. Friedrich, R. van de Krol, N. Guijarro, F. Le Formal and K. Sivula, *Chem. Mater.*, 2017, **29**, 4952-4962.
12. L. Zhang, Y. Li, C. Li, Q. Chen, Z. Zhen, X. Jiang, M. Zhong, F. Zhang and H. Zhu, *ACS nano*, 2017, **11**, 12753-12763.
13. R. R. Prabhakar, W. Septina, S. Siol, T. Moehl, R. Wick-Joliat and S. D. Tilley, *J. Mater. Chem. A*, 2017, **5**, 23139-23145.
14. W. Yang, J. H. Kim, O. S. Hutter, L. J. Phillips, J. Tan, J. Park, H. Lee, J. D. Major, J. S. Lee and J. Moon, *Nat. Commun.*, 2020, **11**, 861.
15. L. Pan, J. H. Kim, M. T. Mayer, M.-K. Son, A. Ummadisingu, J. S. Lee, A. Hagfeldt, J. Luo and M. Gratzel, *Nat. Catal.*, 2018, **1**, 412-420.
16. K. Wang, D. Huang, L. Yu, K. Feng, L. Li, T. Harada, S. Ikeda and F. Jiang, *Acs Catal.*, 2019, **9**, 3090-3097.
17. Y.-X. Yu, L. Pan, M.-K. Son, M. T. Mayer, W.-D. Zhang, A. Hagfeldt, J. Luo and M. Graetzel, *ACS Energy Lett.*, 2018, **3**, 760-766.
18. L. Zhang, Y. Li, X. Li, C. Li, R. Zhang, J.-J. Delaunay and H. Zhu, *Nano Energy*, 2016, **28**, 135-142.
19. F. Wang, W. Septina, A. Chemseddine, F. F. Abdi, D. Friedrich, P. Bogdanoff, R. van de Krol, S. D. Tilley and S. P. Berglund, *J. Am. Chem. Soc.*, 2017, **139**, 15094-15103.

20. H. C. Rojas, S. Bellani, F. Fumagalli, G. Tullii, S. Leonardi, M. T. Mayer, M. Schreier, M. Gratzel, G. Lanzani, F. Di Fonzo and M. R. Antognazza, *Energy Environ. Sci.*, 2016, **9**, 3710-3723.
21. J. Ge, P. J. Roland, P. Koirala, W. Meng, J. L. Young, R. Petersen, T. G. Deutsch, G. Teeter, R. J. Ellingson, R. W. Collins and Y. Yant, *Chem. Mater.*, 2017, **29**, 916-920.